NASA Technical Paper 2440

May 1985

Kinematic Rate Control of Simulated Robot Hand at or Near Wrist Singularity

L. Keith Barker,
Jacob A. Houck,
and Susan W. Carzoo

NASA

NASA
Technical
Paper
2440

1985

Kinematic Rate Control of Simulated Robot Hand at or Near Wrist Singularity

L. Keith Barker
and Jacob A. Houck
Langley Research Center
Hampton, Virginia

Susan W. Carzoo
Sperry Corporation
Hampton, Virginia

National Aeronautics
and Space Administration

**Scientific and Technical
Information Branch**

Abstract

A robot hand should obey movement commands from an operator or a computer program as closely as possible. However, when two of the three rotational axes of the robot wrist are colinear, the wrist loses a degree of freedom, and the usual resolved-rate equations (used to move the hand in response to an operator's inputs) are indeterminant. Furthermore, rate limiting occurs in close vicinity to this singularity. An analysis in this paper shows that rate limiting occurs not only in the vicinity of this singularity but also substantially away from it, even when the operator commands rotational rates of the robot hand that are only a small percentage of the operational joint rate limits. Therefore, joint angle rates are scaled when they exceed operational limits in a real-time simulation of a robot arm. Simulation results show that a small dead band avoids the wrist singularity in the resolved-rate equations but can introduce a high-frequency oscillation close to the singularity. However, when a coordinated wrist movement is used in conjunction with the resolved-rate equations, the high-frequency oscillation disappears.

Introduction

Suppose an operator (human or computer) wants the hand of a robot arm to move in a certain direction. With resolved-rate control (refs. 1 and 2), the operator commands the hand to move with a velocity in that direction. Resolved-rate equations transform the commanded hand velocity into individual joint rates in the robot arm to actually move the hand. Unfortunately, there are certain positions of the robot arm that cause singularities in the equations. At these singularities, the equations are indeterminant, and near them, the equations yield joint angle rates that exceed operational limits. One solution is simply to avoid any positions of the robot arm that cause a singularity. However, in an unplanned maneuver, an operator issues commands to the robot hand, and to move the hand as commanded, the arm may inadvertently pass through a singularity. Undesirable motion may result until the arm moves sufficiently far from the singularity. Consequently, auxiliary equations are needed to continue controlling the robot hand as the arm passes through or near a singular position.

The robot arm configuration shown in figure 1 is used in this paper. The robot hand axis system (X_6, Y_6, Z_6) is translated by the waist, shoulder, and elbow joint angles (θ_1, θ_2, and θ_3, respectively) and is oriented with the robot wrist joint angles (θ_4, θ_5, and θ_6). For this configuration, singularities can occur in either the translational or rotational equations. When the elbow joint angle θ_3 is 0°, the robot arm is fully extended (straightened), and the resolved-rate equations for translational motions are singular. Translational equations have been developed (ref. 3) to move the robot hand at this singular elbow position. The present paper addresses another bothersome singularity, a rotational one involving the robot wrist, that occurs when joint angle rates $\dot{\theta}_4$ and $\dot{\theta}_6$ both produce the same rotation (about Z_6) of the robot hand.

Three rotational joints (4, 5, and 6) in the robot arm constitute the robot wrist. When joints 4 and 6 have their rotational axes colinear, the wrist loses a degree of freedom, and a singularity appears in the resolved-rate equations. Avoiding the singularity (ref. 4) restricts the working space of the hand and requires additional task planning. Use of the generalized matrix inverse to solve the equations (ref. 5) is generally more computationally complex and can yield unwanted hand rotations. For example, in reference 6, it is shown that a commanded rotation about one axis produces a rotation about a different axis. Setting artificial limits or holding previous values (ref. 7) can also cause variations from the desired hand motions. The robot hand should follow the commanded movement as closely as possible, particularly in a delicate task situation, such as handling radioactive material or assisting in the service and repair of a satellite.

A method was introduced in reference 6 to control the robot hand at the wrist singularity. The method uses a coordinated movement (equal magnitudes but opposite directions) of $\dot{\theta}_4$ and $\dot{\theta}_6$ to locate the θ_5 axis in figure 1 for movement of the robot hand in the commanded direction. The present paper is an extension of reference 6. Both analytical and simulation results are presented. New analytical results are given for joint angle rate limiting in the neighborhood of the wrist singularity. In addition, the method is implemented in a real-time simulation of the robot arm (represented graphically on a monitor) which moves in response to an operator's inputs. Moreover, joint angle rates are scaled when they exceed operational limits, and motion of a probe tip in the robot hand is computed for examining deviations from desired hand motions in moving near the wrist singularity.

The primary topics addressed in this paper are (1) the extent of the occurrence of rate limiting in the control of a robot hand by its wrist joints, (2) the use of rate scaling to prevent rate limiting from occurring, and (3) the performance of a proposed coordinated wrist movement in comparison with the usual resolved-rate equations in handling a

wrist singularity. Equations apply to the robot arm in figure 1 and will be different for other configurations; however, the results and basic ideas apply to robot wrists that have three rotational axes passing through a common point.

Symbols

E	elbow of robot arm
G	scaling factor
H	hand of robot arm; origin of hand axis system
i	integer to indicate different axis systems and associated parameters
l_{HW}	length from hand to wrist
M_i	limit on magnitude of rotational rate for joint i
N	neck of robot arm
O	base of robot arm
S	shoulder of robot arm
t	time
V_X, V_Y, V_Z	linear velocity components of robot hand in hand axis system
$(V_X)_c, (V_Y)_c, (V_Z)_c$	commanded linear velocity components of robot hand in hand axis system
W	wrist of robot arm
X_i, Y_i, Z_i	axis system for joint $i + 1$; Z_i is the axis of rotation
$x_{tip}, y_{tip}, z_{tip}$	base coordinates of probe tip
δ_5	upper limit on absolute value of θ_5 in coordinated wrist movement; when magnitude of θ_5 exceeds this limit, resolved-rate equations are used
η	assigned minimum absolute value of $\sin\theta_5$ (eq. (6)) to avoid wrist singularity in resolved-rate equations
θ_i	joint angle with initial value corresponding to position of robot arm in figure 1
$\dot{\theta}_i$	computed joint angle rate for joint i
ω	resultant rotational velocity of robot hand in hand axis system
ω_c	commanded rotational velocity of robot hand in hand axis system
$\omega_X, \omega_Y, \omega_Z$	rotational velocity components of robot hand in hand axis system
$(\omega_X)_c, (\omega_Y)_c, (\omega_Z)_c$	commanded rotational velocity components of robot hand in hand axis system
$\omega_{1,2,3}$	rotational velocity of robot hand caused by rotation of joints 1, 2, and 3 in hand axis system
$\omega_{4,5,6}$	rotational velocity of robot hand caused by rotation of three wrist joints 4, 5, and 6 in hand axis system

leveloneAnalysis

The robot arm with axis systems is shown in figure 1. The axis system chosen for operator inputs is the robot hand axis system (X_6, Y_6, Z_6). It is assumed that $l_{HW} = 0$ to locate the origin of the hand axis system at the intersection of the rotational axes of the robot wrist. Thus, wrist rotation (θ_4, θ_5, and θ_6) does not translate the origin of the hand axis system. The diagram in figure 2 indicates the control of the robot arm by kinematic resolved-rate equations, which are partitioned as (1) translational velocity equations (waist, shoulder, and elbow) that translate the robot hand and (2) rotational velocity equations (wrist) that orient the robot hand. Singularities in the translational equations are considered in other references (refs. 2, 3, 5, and 7). The commanded linear velocity components $(V_X)_c$, $(V_Y)_c$, and $(V_Z)_c$ yield the joint angle rates $\dot{\theta}_1$, $\dot{\theta}_2$, and $\dot{\theta}_3$. The commanded rotational velocity components $(\omega_X)_c$, $(\omega_Y)_c$, and $(\omega_Z)_c$, along with the computed joint angle rates $\dot{\theta}_1$, $\dot{\theta}_2$, and $\dot{\theta}_3$, yield the wrist joint angle rates $\dot{\theta}_4$, $\dot{\theta}_5$, and $\dot{\theta}_6$. The robot arm joint angle rates are then integrated to get the next set of joint angles for movement of the robot arm. Using visual feedback (movement of a graphical robot arm on a monitor), the operator varies his commands.

Resolved-Rate Equations for Robot Wrist

The resultant rotational velocity of the robot hand (in the hand axis system), caused by the six rotational joints in the robot arm, is

$$\omega = \omega_{1,2,3} + \omega_{4,5,6} \tag{1}$$

where $\omega_{1,2,3}$ is the rotational velocity caused by the first three joints (waist, shoulder, elbow) in the robot arm, and $\omega_{4,5,6}$ is the rotational velocity caused by the three wrist joints. An operator commands the desired rotational velocity ω_c in the hand axis system. With $\omega = \omega_c$, equation (1) gives the necessary wrist joint angle velocity as

$$\omega_{4,5,6} = \omega_c - \omega_{1,2,3} \tag{2}$$

Notice that $\omega_{1,2,3}$ simply modifies the commanded rotational velocity ω_c. Expressions for $\omega_{1,2,3}$ are found in reference 6. In the present paper, assume $\omega_{1,2,3} = 0$, which means the robot hand axis system is not translated by the waist, shoulder, or elbow joint angles (θ_1, θ_2, and θ_3, respectively). Then, in scalar form, equation (2) relates wrist joint angle rates to commanded rotational rates as (ref. 6)

$$\dot{\theta}_5 = (\omega_X)_c \sin\theta_6 + (\omega_Y)_c \cos\theta_6 \tag{3}$$

$$\dot{\theta}_4 = \frac{-(\omega_X)_c \cos\theta_6 + (\omega_Y)_c \sin\theta_6}{\sin\theta_5} \tag{4}$$

$$\dot{\theta}_6 = (\omega_Z)_c - \dot{\theta}_4 \cos\theta_5 \tag{5}$$

When $\theta_5 = 0°$, the colinearity of the wrist rotational axes Z_3 and Z_5 in figure 1 causes the wrist to lose a degree of freedom. In equation (4), $\dot{\theta}_4 \to \infty$ as $\theta_5 \to 0°$. The problem is to control the robot hand as it is commanded at or near this singularity ($\theta_5 = 0°$).

Equations (3) to (5) are the resolved-rate equations for the wrist joint angle rates to rotate the robot hand. The denominator term in equation (4) is replaced by

$$\sin\theta_5 = \eta \ \mathrm{sgn}(\sin\theta_5) \tag{6}$$

whenever $|\sin\theta_5| < \eta$ to avoid an indeterminant condition or arithmetic overflow in the vicinity of the robot wrist singularity $\theta_5 = 0°$. That is, when the absolute value of $\sin\theta_5$ is less than η, $\sin\theta_5$ is assigned the value η times the algebraic sign of $\sin\theta_5$. Different values of η are examined in a later section of this paper.

Rate-Limiting Borderlines When Robot Wrist Is Controlled by Resolved-Rate Equations

Physically, joints in the robot wrist can rotate only so fast, even if as the wrist singularity is approached ($\theta_5 \to 0°$), the computed joint angle rates $\dot{\theta}_4$ and $\dot{\theta}_6$ (eqs. (4) and (5)) are very large. Rate limiting occurs when an operator input results in a computed joint angle rate that exceeds the operational limit of that joint, and the associated joint responds by moving at its fastest allowable rate. Reference 6 shows that if rate limiting occurs, then unwanted hand movements can result.

Commanded rotational robot hand rate $(\omega_X)_c$. Consider rate limiting on wrist joint 4 due to $(\omega_X)_c$. With $(\omega_Y)_c = 0$, nondimensionalize equation (4) as

$$\frac{-(\omega_X)_c}{M_4} = \frac{\dot{\theta}_4}{M_4} \frac{\sin\theta_5}{\cos\theta_6} \tag{7}$$

where M_4 is the limiting (maximum magnitude) rotational rate of joint 4. Taking the magnitude of equation (7) gives

$$\frac{|(\omega_X)_c|}{M_4} = \frac{|\dot{\theta}_4|}{M_4} \left| \frac{\sin\theta_5}{\cos\theta_6} \right| \tag{8}$$

When the operational limit is reached, $|\dot{\theta}_4| = M_4$ and equation (8) becomes

$$\frac{|(\omega_X)_c|}{M_4} = \left| \frac{\sin\theta_5}{\cos\theta_6} \right| \tag{9}$$

The nondimensional magnitude of the operator's commanded input $(\omega_X)_c$ in equation (9) is a function of the magnitudes of the wrist joint angles θ_5 and θ_6 and, by design, is on the borderline of causing rate limiting to occur on joint 4. (Larger values will cause rate limiting.) Thus, for given values of θ_5 and θ_6, equation (9) gives the maximum magnitude of operator input which can be used without causing rate limiting on joint 4.

The left side of equation (9) in percent is plotted in figure 3(a) as a function of $|\theta_5|$ for specified values of $|\theta_6|$. As an example, if $\theta_6 = 0°$ and $\theta_5 = 10°$, rate limiting will occur whenever the magnitude of the commanded robot hand rate $(\omega_X)_c$ exceeds about 17 percent of the maximum allowable joint rate magnitude for joint 4.

Similarly, rate-limiting borderlines due to $(\omega_X)_c$ are established for wrist joint 6. With $(\omega_Y)_c = 0$ and $(\omega_Z)_c = 0$, solving equation (5) for $\dot{\theta}_4$, substituting into equation (7), replacing M_4 with M_6 (the maximum rotational rate magnitude for joint 6) to nondimensionalize, and taking the magnitude ($|\dot{\theta}_6| = M_6$) yields

$$\frac{|(\omega_X)_c|}{M_6} = \left| \frac{\tan\theta_5}{\cos\theta_6} \right| \tag{10}$$

The left side of equation (10) in percent is plotted in figure 3(b) as a function of $|\theta_5|$ for specified values of

$|\theta_6|$. With $\theta_6 = 0°$ and $\theta_5 = 10°$, rate limiting will occur whenever the magnitude of the commanded robot hand rate $(\omega_X)_c$ exceeds about 17 percent of the maximum allowable joint rate magnitude for joint 6 with $(\omega_Y)_c = (\omega_Z)_c = 0$.

Commanded rotational robot hand rate $(\omega_Y)_c$. An equation for rate-limiting borderlines due to $(\omega_Y)_c$ is obtained for joint 4 from equation (4) with $(\omega_X)_c = 0$ and $|\dot{\theta}_4| = M_4$ as

$$\frac{|(\omega_Y)_c|}{M_4} = \left|\frac{\sin\theta_5}{\sin\theta_6}\right| \tag{11}$$

where, once again, M_4 is the operational rate-limiting magnitude for joint 4. The left side of equation (11) in percent is plotted in figure 3(c) as a function of $|\theta_5|$ for specified values of $|\theta_6|$.

Rate-limiting borderlines due to $(\omega_Y)_c$ are generated for joint 6 by the equation

$$\frac{|(\omega_Y)_c|}{M_6} = \left|\frac{\tan\theta_5}{\sin\theta_6}\right| \tag{12}$$

With $(\omega_X)_c = (\omega_Z)_c = 0$, equation 12 is obtained by solving equation (5) for $\dot{\theta}_4$, substituting this expression into equation (4), solving equation (4) for $(\omega_Y)_c$, nondimensionalizing by M_6 (the limit on the joint angle rate magnitude for joint 6), and taking the magnitude ($|\dot{\theta}_6| = M_6$). The left side of equation (12) in percent is plotted in figure 3(d) as a function of $|\theta_5|$ for specified values of $|\theta_6|$.

The basic message in figure 3 is that rate limiting occurs for large wrist joint angles even when the operator commands rotational rates of the robot hand that are only a small percentage of the maximum allowable joint rate limit. For example, let the joint angle rate limit on joint 6 be $M_6 = 28.6$ deg/sec (0.5 rad/sec). Then, if $\theta_6 = 90°$ and $\theta_5 = 12°$ in figure 3(d), the operator command $(\omega_Y)_c$ must not exceed approximately 5.7 deg/sec (0.1 rad/sec) in magnitude, or rate limiting will occur. These results illustrate the possible wide range of occurrence of rate limiting and the consequent need to incorporate rate scaling into the practical control of robot arms.

Scaling Joint Angle Rates

The operator's inputs ω_c can be scaled so that no calculated joint angle rate exceeds its operational limit to avoid the rate-limiting problem in resolved-rate control near the wrist singularity. However, scaling the computed wrist joint angle rates $\dot{\theta}_4$, $\dot{\theta}_5$, and $\dot{\theta}_6$ from equations (3), (4), and (5) by a scale factor G gives the same result as scaling the operator inputs $(\omega_X)_c$, $(\omega_Y)_c$, and $(\omega_Z)_c$ by G and recomputing the joint rates.

With M_i denoting the limit on the rotational rate magnitude of joint i, a scaling procedure for the wrist joints is indicated in the following steps:

Step 1: Calculate the wrist joint angle rates $\dot{\theta}_4$, $\dot{\theta}_5$, and $\dot{\theta}_6$.

Step 2: If the calculated joint angle rates are within their limits ($|\dot{\theta}_i| \leq M_i$ for $i = 4$, 5, and 6), use these calculated rates; otherwise, go to step 3.

Step 3: Multiply the calculated joint angle rates in step 1 by the scaling factor

$$G = \frac{M_k}{|\dot{\theta}_k|} \tag{13}$$

where $\dot{\theta}_k$ is the calculated joint angle rate that most exceeds its limit M_k.

In step 3, the calculated joint angle rate that most exceeds its limit is scaled to equal its limit. This means that the other calculated joint angle rates will also be scaled by G to fall within their operational limits. The joint angle rates $\dot{\theta}_1$, $\dot{\theta}_2$, and $\dot{\theta}_3$ translate the origin of the robot hand axis system and can also be included in the scaling process; however, in this study, these rates are assumed to be zero.

Coordinated Wrist Movement To Rotate Robot Hand

When the robot wrist is positioned with $\theta_5 = 0°$ (fig. 1), equation (4) is indeterminant. However, use of equation (6) allows computations to continue. Another way to rotate the robot hand at the singularity is to use the coordinated wrist movement in reference 6. In this method, joint angles θ_4 and θ_6 are varied at maximum rates, but in opposite directions, to keep the robot hand stationary. A stationary hand is necessary for a smooth nondisruptive movement through the singularity. This coordinated movement is stopped when Z_4 is positioned so that the hand can be moved as commanded with $\dot{\theta}_5$. Thus, as soon as operationally possible, the robot hand will move as commanded. As the robot wrist moves away from the singularity, the resolved-rate equations are used. The coordinated wrist movement is used whenever

$$|\theta_5| < \delta_5 \tag{14}$$

where δ_5 is a specified constant. In this paper, $\delta_5 = 0.01°$ (1.75×10^{-4} rad). In the coordinated wrist movement (ref. 6), logic is provided to choose the least rotation of joints 4 and 6 that will position the robot hand for movement by $\dot{\theta}_5$ without violating any operational limits. This logic does not exist

in the usual resolved-rate equations. Later in this paper, an example is given in which a commanded hand rotation is possible with the coordinated wrist movement, but not with the resolved-rate equations when there are joint angle limits.

Probe Tip

The origin H of the hand axis system, rather than being displaced as shown in figure 1, is chosen to coincide with W (intersection of the robot wrist rotational axes Z_3, Z_4, and Z_5); therefore, wrist rotations do not translate the origin of the hand axis system. However, the movement of the tip of a probe in the robot hand is used to examine deviations from ideal movements during robot wrist rotation. The length of the probe is assumed to be 188 mm and to lie along Z_6 in figure 1. Base coordinates of the probe tip are denoted by x_{tip}, y_{tip}, and z_{tip} (appendix).

Results and Discussion

The robot arm in figure 1 is kinematically simulated, and a graphical representation of the arm (ref. 8) moves in real time on a monitor in response to an operator's commands. The simulation was conducted on a Control Data CYBER 175 computer with an Adams-Bashforth second-order predictor integration algorithm having an integration step size of 1/32 sec. The primary interest in this paper is the rotation of the robot hand by its wrist joints in response to the operator's rotational velocity commands $(\omega_X)_c$, $(\omega_Y)_c$, and $(\omega_Z)_c$. Slower, more accurate hand movements are preferred over faster, erroneous movements.

Basic Test Maneuver

Relative to the robot arm in figure 1, a basic test maneuver is defined as a rotation of the robot hand about X_6. An operator issues the single rotational command $(\omega_X)_c$ for the value of ω_X. During the maneuver, $\theta_1 = \theta_2 = \theta_3 = 0°$. The initial position corresponds to the robot wrist singularity ($\theta_5 = 0°$) in the resolved-rate equations. Equation (6) is used to avoid an indeterminant condition. The operator commands $(\omega_X)_c$ values sufficiently large to cause the wrist joints to rotate at their assumed maximum allowable rates (28.6 deg/sec or 0.5 rad/sec). Data from this maneuver for two different control schemes (resolved rate and resolved rate with coordinated wrist movement) are compared for joint angle rates, joint angle movements, and probe tip movement.

Five values of η are used in examining the basic maneuver. Data for probe x_{tip} movement are plotted to illustrate the effects of η.

Using Resolved-Rate Equations in Test Maneuver

Equations (3) to (5) (the resolved-rate equations) and equation (6) are used to compute the joint angle rates for the robot wrist in response to the basic test-maneuver command ($(\omega_X)_c = 0.5$ rad/sec). These rates are integrated to get the wrist joint angles, which are used in equation (A1), to compute the movement of the probe tip in base coordinates. Figure 4 shows the resulting joint angle rates and joint angles when a dead-band value of $\eta = 10^{-5}$ is used. Figure 5 shows the resulting movement of the probe tip in comparison with the ideal movement for the test maneuver.

In figure 4(a), joints 4 and 6 counterrotate until slightly beyond 3 sec, at which time an undesirable oscillation occurs. After the oscillation subsides, joint 5 tilts the robot hand. Figure 4(b) shows a small-amplitude oscillation in joint angles θ_4 and θ_6 corresponding to the oscillation in figure 4(a). Joint angle θ_4 moves to $-90°$ while θ_6 moves to 90°; afterwards θ_5 tilts the robot hand to 95° (joint angle limit).

Figure 5 shows a comparison of probe tip movement for the ideal and the resolved-rate equations. (Also shown are results for the resolved-rate equations with coordinated wrist movement, which will be discussed later.) Ideally, the x-coordinate of the probe tip should remain zero throughout the test maneuver. However, figure 5(a) shows an oscillation and slight deviation from the ideal. The y-coordinate (fig. 5(b)) and z-coordinate (fig. 5(c)) differ from the ideal by slightly over 3 sec. Figure 5(d) shows that the difference between the ideal and actual y_{tip} as a function of z_{tip} is zero; therefore, the probe tip travels the same path in the y-z plane, except for the 3-sec delay in transit time along this path. The undesirable oscillation in figure 4(a) can be eliminated by relaxing the dead band η, but this results in more uncommanded movement of the probe tip. To show the effect on the resolved-rate equations of various values for the dead band η (eq. (6)), the basic maneuver was examined for five values of η: 10^{-5}, 10^{-4}, 10^{-3}, 10^{-2}, and 10^{-1}. The variation of the probe tip x-coordinate for each value of η was compared with the ideal. Although relaxing the dead band η helps eliminate the undesirable oscillations seen in figure 4(a), care must be taken that undesired and uncommanded movement of the probe tip is not introduced. Figure 6 illustrates the increase in undesired movement as the value for η is relaxed (i.e., as η is increased).

Using Resolved-Rate Equations and Coordinated Wrist Movement in Test Maneuver

The coordinated wrist movement is used in the vicinity ($|\theta_5| < \delta_5$, where $\delta_5 = 0.01°$) of the wrist singularity $\theta_5 = 0°$. Outside this region, the regular resolved-rate equations (eqs. (3) to (5)) with the dead band (eq. (6)) are used. Figure 7 shows the joint angle rates and joint angles for wrist movement in the test maneuver. The undesirable oscillations that appeared in figure 4 are not present in figure 7. Figure 5 shows the corresponding probe tip coordinates in comparison with those for the ideal and the resolved-rate equations.

The probe tip movement is identical to the ideal test maneuver, except for a time delay of slightly over 3 sec caused by the rotation of joints 4 and 6.

Additional Movement Capability From Wrist Singularity ($\theta_5 = 0°$)

Let the joint angle θ_4 be limited by $|\theta_4| \leq 135°$. Now, consider the execution of the basic maneuver (positive rotation about X_6 when the starting wrist joint angles are $\theta_4 = -130°$ and $\theta_5 = \theta_6 = 0°$. Figure 8 shows the results for resolved-rate equations, and figure 9 shows the results for resolved-rate equations with coordinated wrist movement. The resolved-rate equations yield a negative value for $\dot{\theta}_4$ because the logic is not present that θ_4 cannot be rotated negatively through the joint angle limit $-135°$; therefore, θ_4 varies from $-130°$ to $-135°$ and stops. However, the equations for the joint angle rates with the coordinated wrist movement do contain this logic; hence, $\dot{\theta}_4$ varies positively and $\dot{\theta}_6$ negatively to accomplish the commanded hand movement. However, if the starting wrist position is the same as before, except joint 5 is outside the dead band (eq. (14)) where the coordinated wrist movement is used, then the basic maneuver cannot be accomplished. The dead band could be increased to allow the maneuver, but when Z_6 and Z_3 (fig. 1) are not colinear, the robot hand will move during the coordinated wrist movement. A better solution would be to design joints 4 and 6 for extended rotational capability, so that the resolved-rate equations can be used outside a small dead band of the wrist singularity without encountering a joint limit that prevents further movement of the robot hand in a desired direction. Thus, incorporating the coordinated wrist movement offers some extended movement capability when joint angle limits exist.

Conclusions

The practical application of resolved-rate control theory to teleoperator robot arms has encountered several difficulties. In this paper, rate limiting was shown to occur with greater frequency than anticipated. As a result, rate scaling was suggested and analyzed as an integral element of controlling a teleoperator robot arm. That is, operator control inputs were scaled within maximum rate limits to allow a more acceptable system response to the frequent occurrence of rate limiting. However, this technique still does not solve the movement difficulty associated with a wrist singularity in the resolved-rate equations. Previous methods of robotic control at a wrist singularity have had limitations or adverse side effects; therefore, a new method (coordinated wrist movement) was investigated and found to have advantages compared with previous methods. A robot arm was kinematically simulated, and a graphical representation of the arm moved in real time on a monitor in response to an operator's commands.

With respect to robot hand control by its wrist joints, the following specific conclusions are drawn:

1. The percentage of the maximum joint angle rate that an operator can obtain is related to how close the robot wrist is to the singularity. For example, analytical results show that even as much as 10° away from the wrist singularity, this percentage can be as low as approximately 17 percent. Therefore, joint angle rates must be scaled in resolved-rate control to avoid rate limiting.

2. A dead band avoids the wrist singularitv in the resolved-rate equations, but simulation results show that a small dead band leads to a high-frequency oscillation when close to the singularity, whereas a larger dead band leads to erroneous hand movements.

3. A coordinated wrist movement of joints 4 and 6 of the robot wrist to locate joint 5 for movement of the robot hand in the commanded direction appears to enhance the dexterity of the robot arm at the wrist singularity. (Rotational axes of joints 4 and 6 are colinear.) Simulation results show that there is no high-frequency oscillation, and except for a brief delay for the coordinated wrist movement, the robot hand moves as commanded.

4. When limits exist on the wrist joint angles, the coordinated wrist movement can allow the robot hand to perform a maneuver from the wrist singularity that cannot be performed by the resolved-rate equations. It appears that joints 4 and 6 should be designed for extended rotational capability to prevent encountering joint limits that prevent further movement of the robot hand in a desired direction.

NASA Langley Research Center
Hampton, VA 23665
February 22, 1985

Appendix

Movement of Probe Tip in Robot Hand With Respect to Base Coordinate System

Additional symbols used in this appendix are defined as follows:

C_i $= \cos\theta_i$

C_{23} $= \cos(\theta_2 + \theta_3)$

$\mathbf{L}$ transformation matrix (rotational part) from hand coordinate system to base coordinate system

l_{ES} length from elbow to shoulder

l_{NO} length from neck to base

l_{SN} length from shoulder to neck

l_{WE} length from wrist to elbow

$\mathbf{p}_{06}$ vector in base coordinates from origin of base coordinate system to origin of hand axis system

$\mathbf{q}_0$ vector in base coordinates from origin of base coordinate system to tip of probe in robot hand

$\mathbf{q}_6$ vector in hand coordinates from origin of hand coordinate system to tip of probe in robot hand

S_i $= \sin\theta_i$

S_{23} $= \sin(\theta_2 + \theta_3)$

Let $\mathbf{q}_6$ be a vector to the tip of a probe in the robot hand axis system. Let $\mathbf{q}_0$ be the vector location of this same point with respect to the base coordinate system. Then,

$$\mathbf{q}_0 = \mathbf{L}\mathbf{q}_6 + \mathbf{p}_{06} \tag{A1}$$

where $\mathbf{L}$ is a rotational transformation matrix (ref. 3) and $\mathbf{p}_{06}$ is the position vector in base coordinates from the base coordinate system to the robot hand coordinate system.

With the robot arm parameters in reference 5, the equation for $\mathbf{p}_{06}$ in reference 9 becomes

$$\mathbf{p}_{06} = \begin{Bmatrix} C_1(S_{23}l_{WE} + S_2 l_{ES}) - S_1 l_{SN} \\ S_1(S_{23}l_{WE} + S_2 l_{ES}) + C_1 l_{SN} \\ C_{23}l_{WE} + C_2 l_{ES} + l_{NO} \end{Bmatrix} \tag{A2}$$

In this paper, the coordinates of the tip of the hand probe in base coordinates are denoted as x_{tip}, y_{tip}, and z_{tip}; that is

$$\mathbf{q}_0 = \begin{Bmatrix} x_{tip} \\ y_{tip} \\ z_{tip} \end{Bmatrix} \tag{A3}$$

The probe is assumed to be 188 mm long and to lie along Z_6 in figure 1. Hence,

$$\mathbf{q}_6 = \begin{Bmatrix} 0 \\ 0 \\ 188 \end{Bmatrix} \tag{A4}$$

Other distances assumed in this paper are $l_{NO} = 660$ mm, $l_{ES} = l_{WE} = 432$ mm, and $l_{SN} = 152$ mm.

References

1. Whitney, Daniel E.: Resolved Motion Rate Control of Manipulators and Human Prostheses. *IEEE Trans. Man-Mach. Syst.*, vol. MMS-10, no. 2, June 1969, pp. 47–53.
2. Whitney, D. E.: The Mathematics of Coordinated Control of Prosthetic Arms and Manipulators. *J. Dyn. Syst., Meas., & Control*, vol. 94, ser. G, no. 4, Dec. 1972, pp. 303–309.
3. Barker, L. Keith; Houck, Jacob A.; and Carzoo, Susan W.: *Translational Control of a Graphically Simulated Robot Arm by Kinematic Rate Equations That Overcome Elbow Joint Singularity.* NASA TP-2376, 1984.
4. Paul, Richard P.; and Stevenson, Charles N.: Kinematics of Robot Wrists. *Int. J. Robotics Res.*, vol. 2, no. 1, Spring 1983, pp. 31–38.
5. Yeh, Shao-Chi: Locomotion of a Three-Legged Robot Over Structural Beams. M.S. Thesis, Ohio State Univ., Aug. 1981.
6. Barker, L. Keith; and Moore, Mary C.: *Kinematic Control of Robot With Degenerate Wrist.* NASA TP-2341, 1984.
7. Klein, Charles A.; and Patterson, Mark R.: Computer Coordination of Limb Motion for Locomotion of a Multiple-Armed Robot for Space Assembly. *IEEE Trans. Syst., Man, and Cybern.*, vol. SMC-12, no. 6, Nov./Dec. 1982, pp. 913–919.
8. Pennington, Jack E.: *A Rate-Controlled Teleoperator Task With Simulated Transport Delays.* NASA TM-85653, 1983.
9. Barker, L. Keith: *Kinematic Equations for Resolved-Rate Control of an Industrial Robot Arm.* NASA TM-85685, 1983.

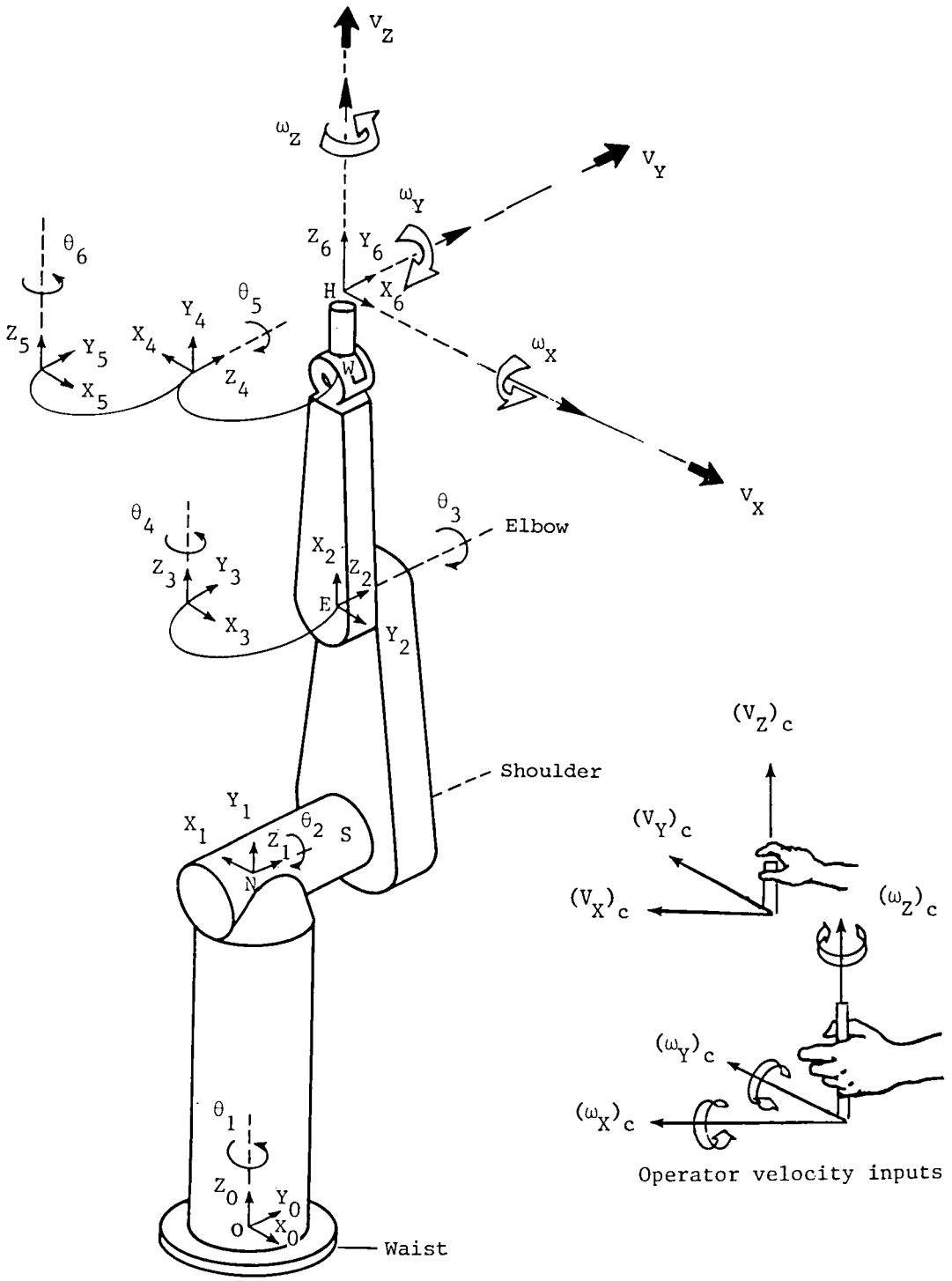

Figure 1. Initial position of robot arm, joint axis systems, and commanded robot hand velocities.

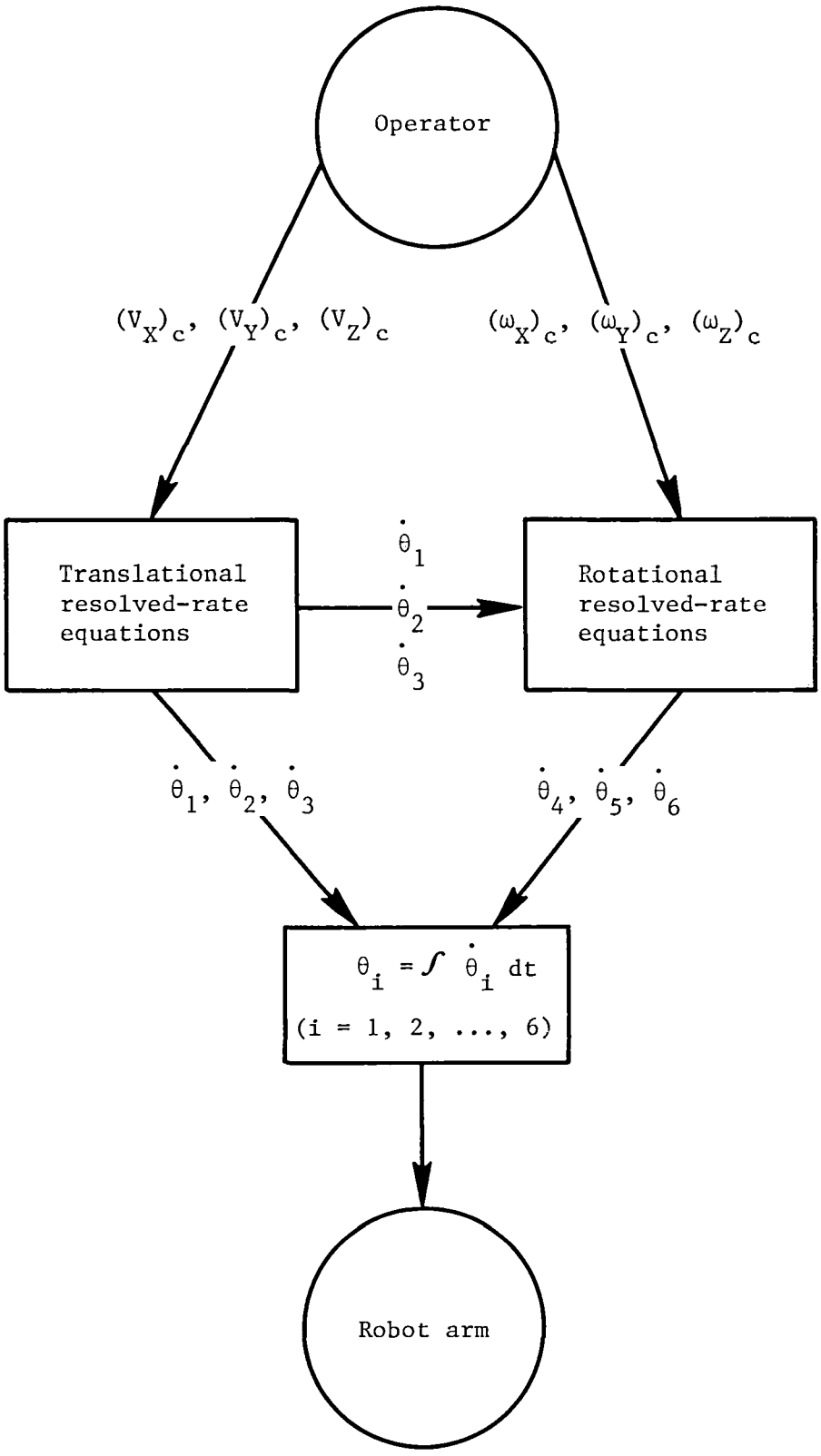

Figure 2. Diagram used to discuss control of robot arm by kinematic resolved-rate equations.

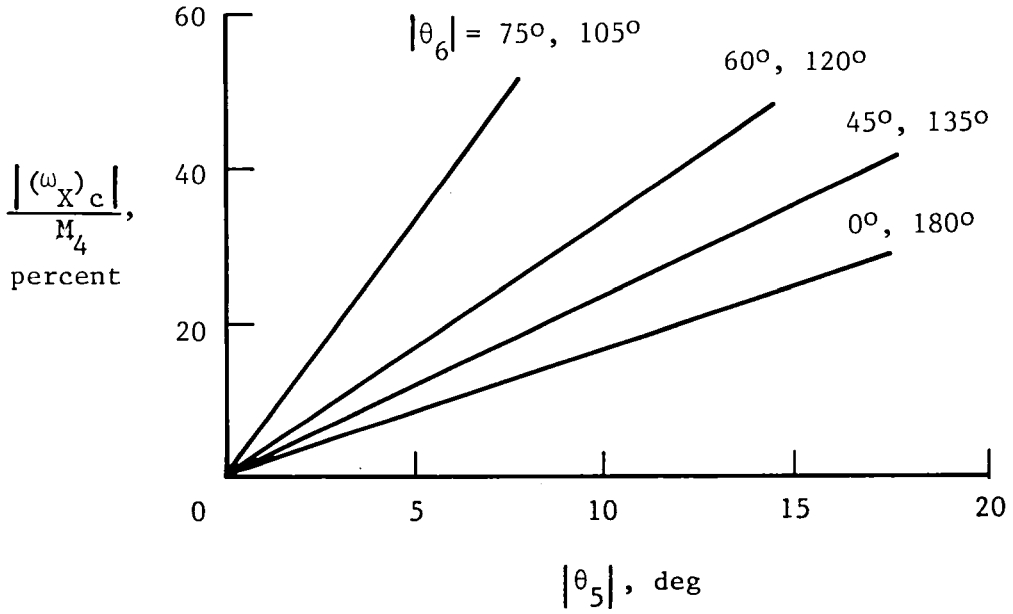

(a) Rate limiting on wrist joint 4; $(\omega_Y)_c = 0$.

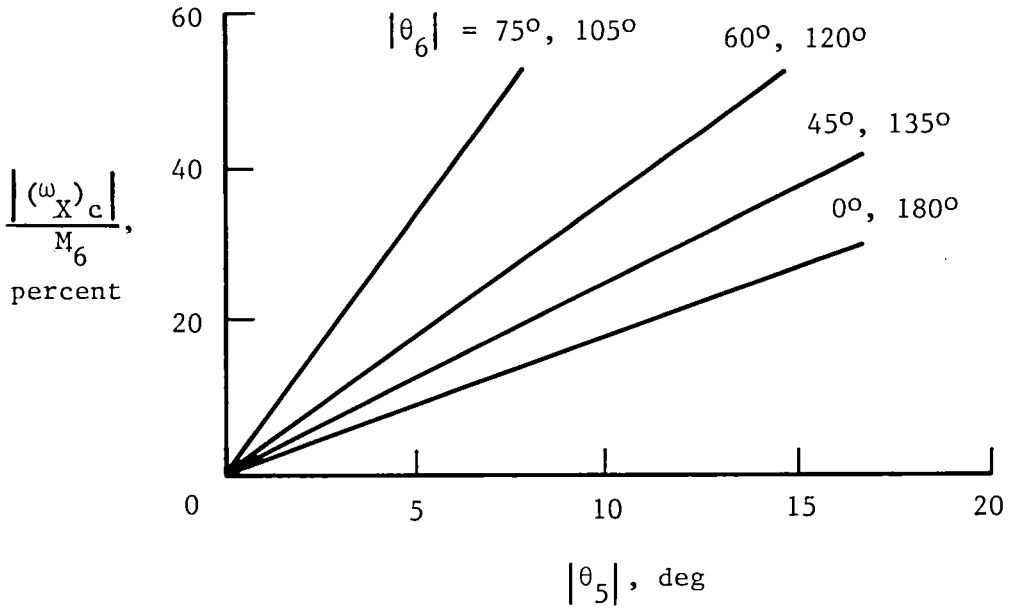

(b) Rate limiting on wrist joint 6; $(\omega_Y)_c = (\omega_Z)_c = 0$.

Figure 3. Commanded robot hand rotations on borderlines of causing rate limiting.

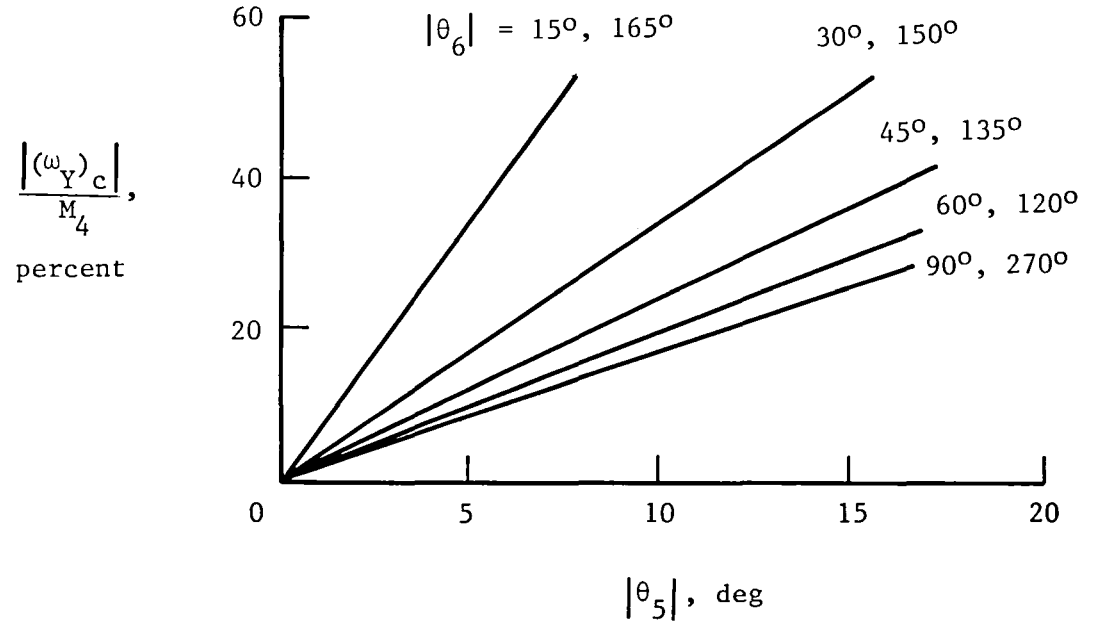

(c) Rate limiting on wrist joint 4; $(\omega_X)_c = 0$.

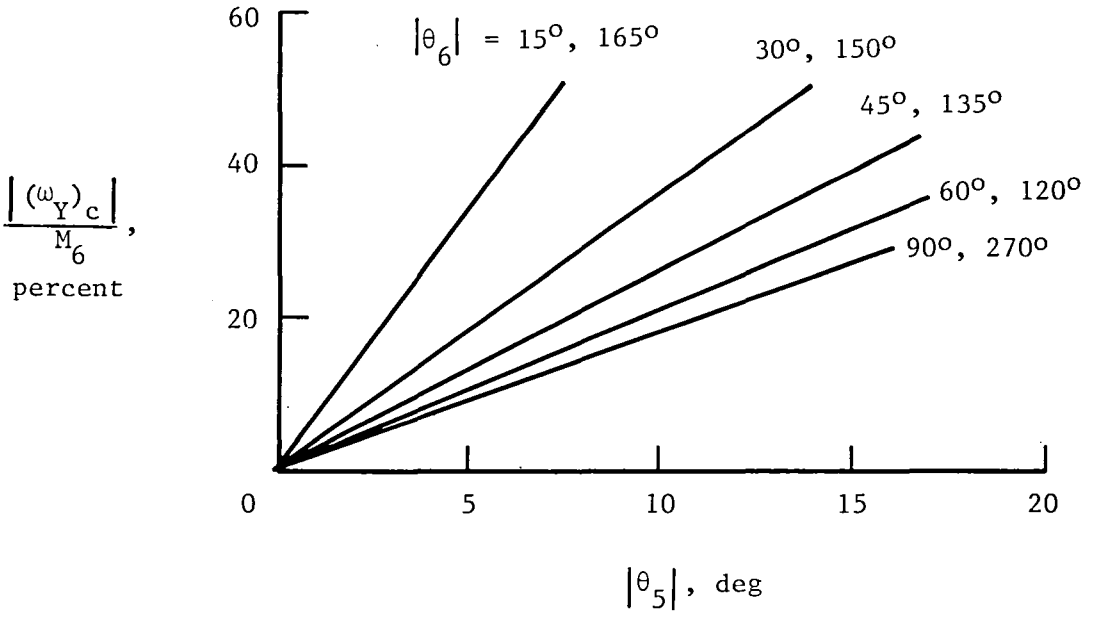

(d) Rate limiting on wrist joint 6; $(\omega_X)_c = (\omega_Z)_c = 0$.

Figure 3. Concluded.

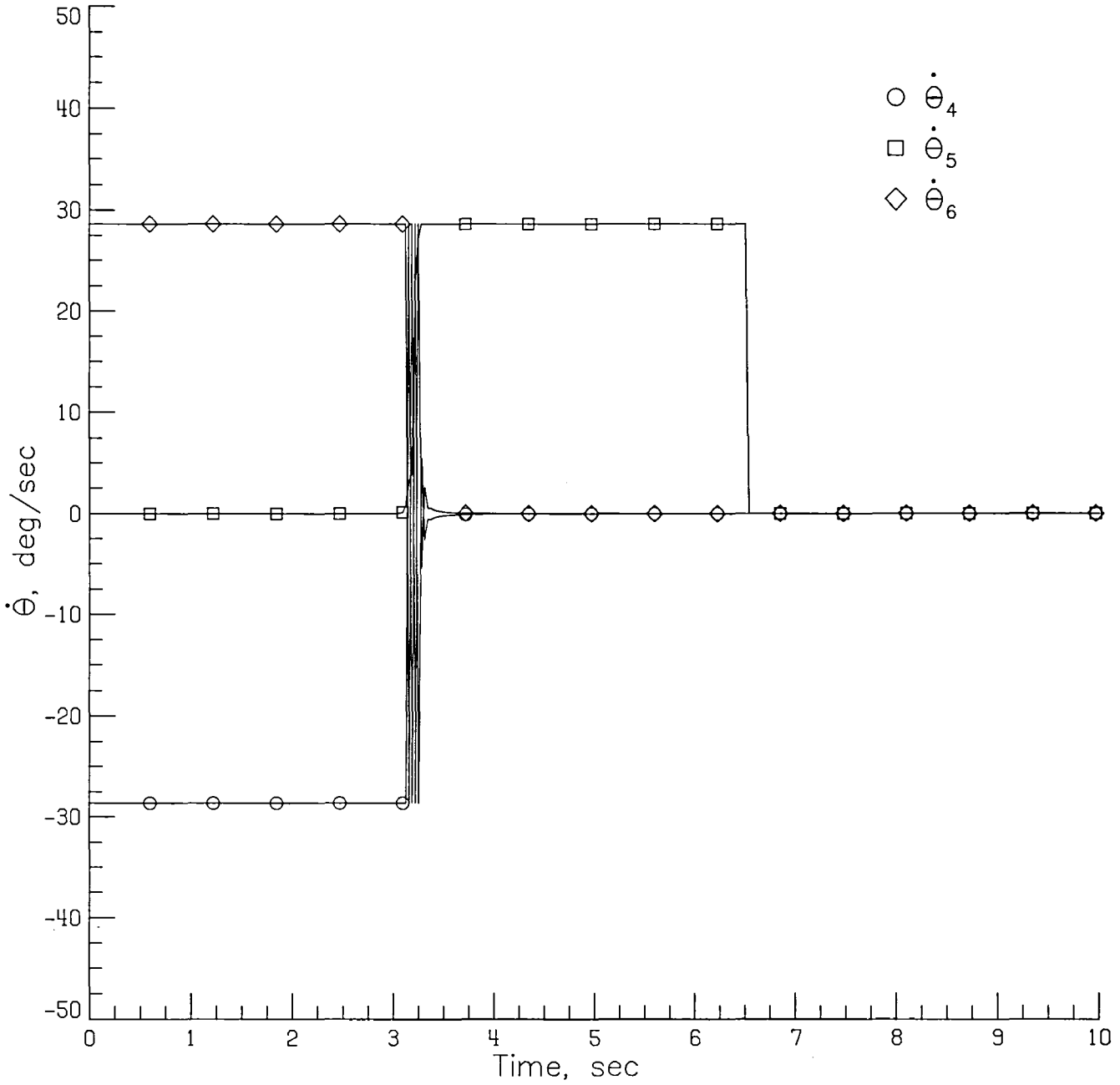

(a) Joint angle rates.

Figure 4. Joint angle rates and joint angles during test maneuver using resolved-rate equations. $\eta = 10^{-5}$.

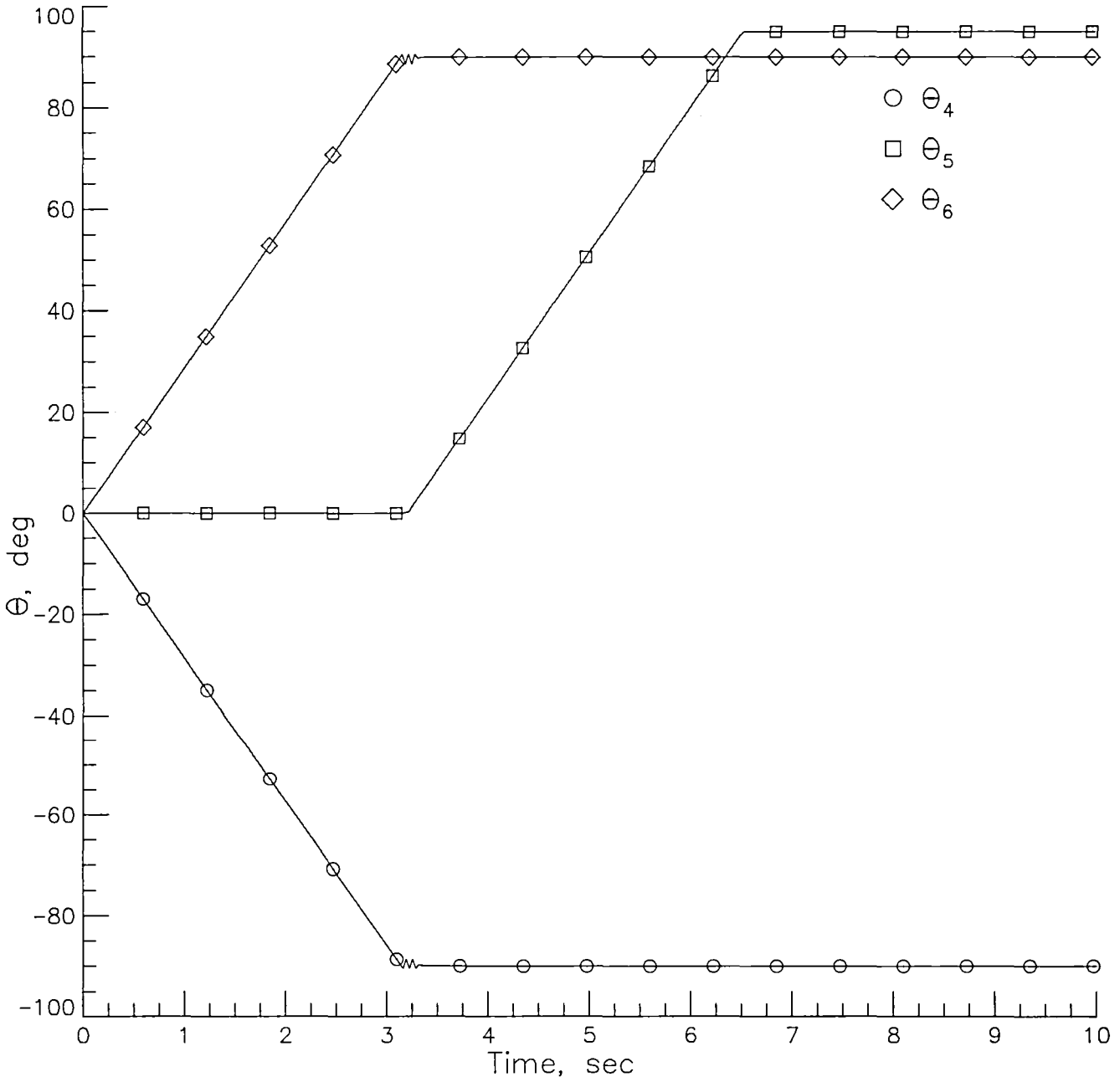

(b) Joint angles.

Figure 4. Concluded.

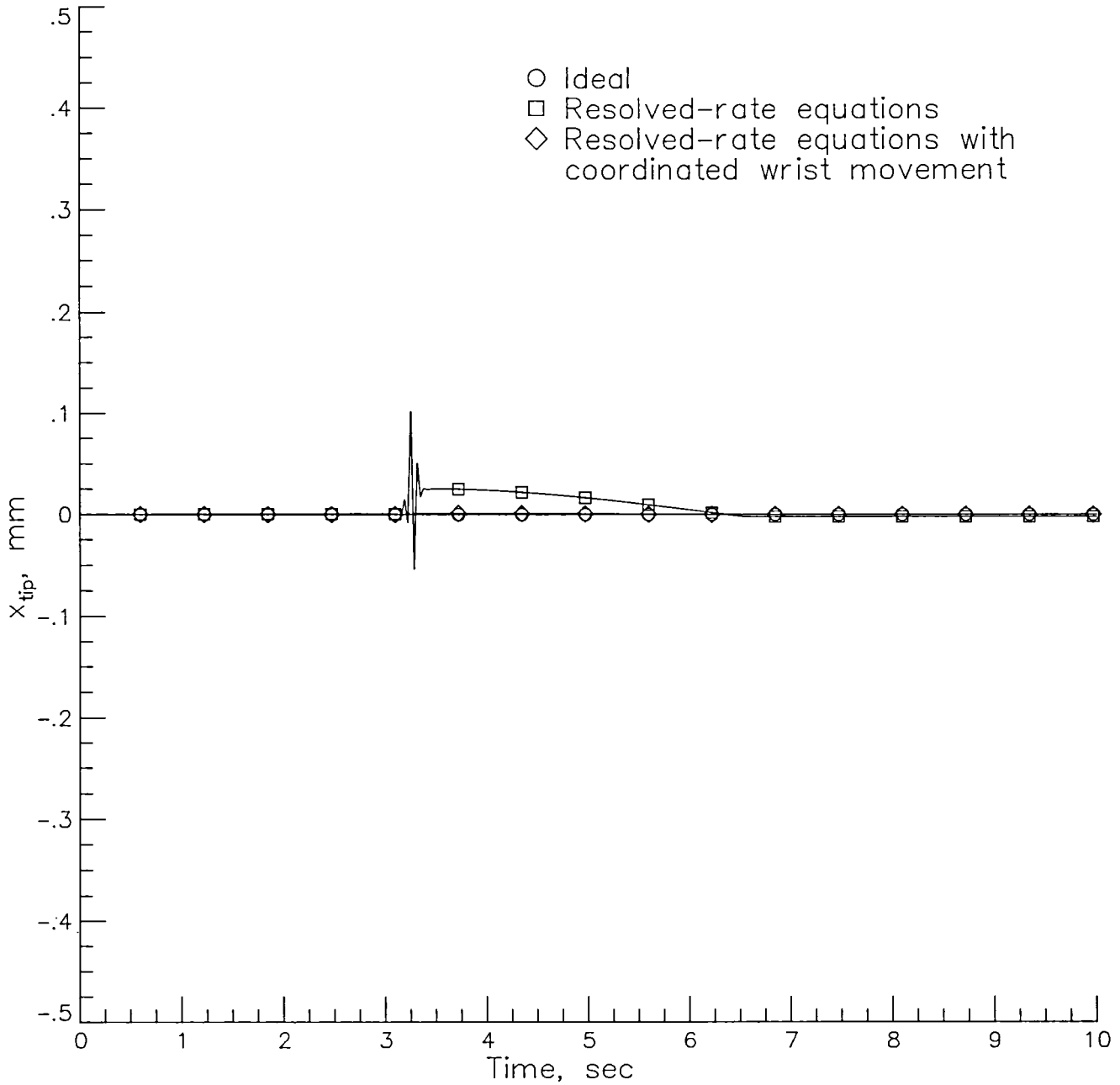

(a) x-coordinate of probe tip.

Figure 5. Comparison of probe tip coordinates during test maneuver. $\eta = 10^{-5}$.

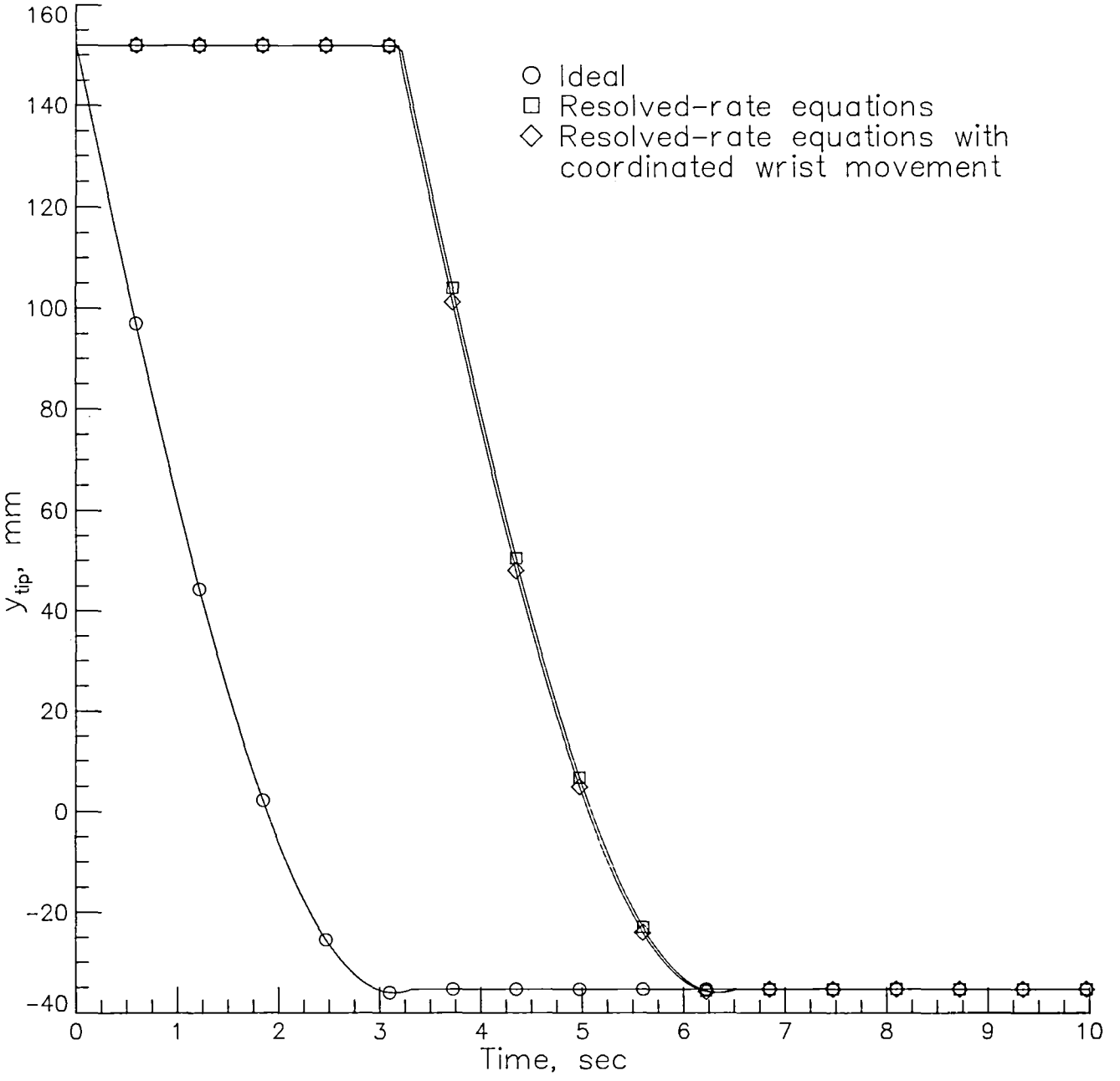

(b) y-coordinate of probe tip.

Figure 5. Continued.

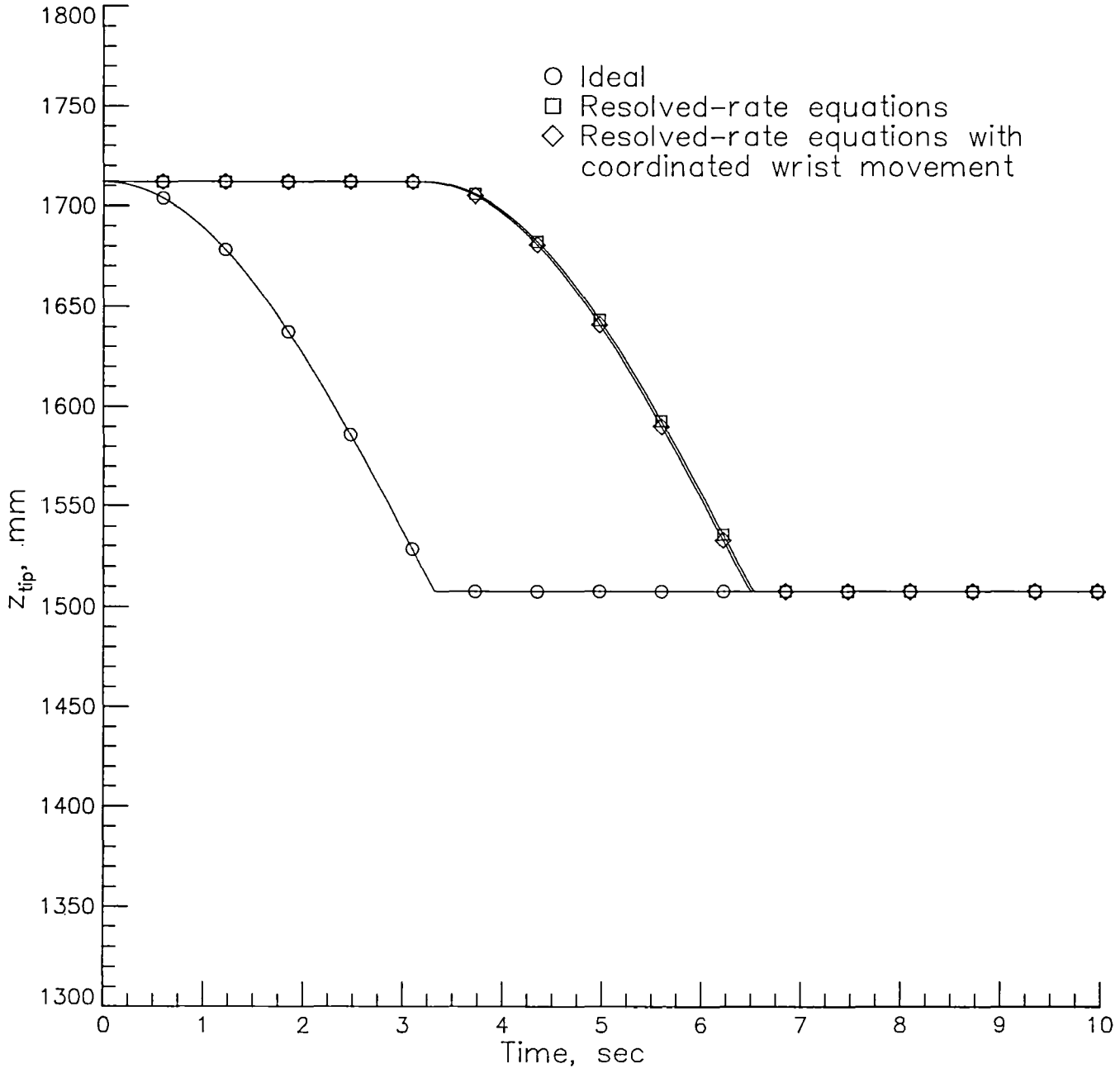

(c) z-coordinate of probe tip.

Figure 5. Continued.

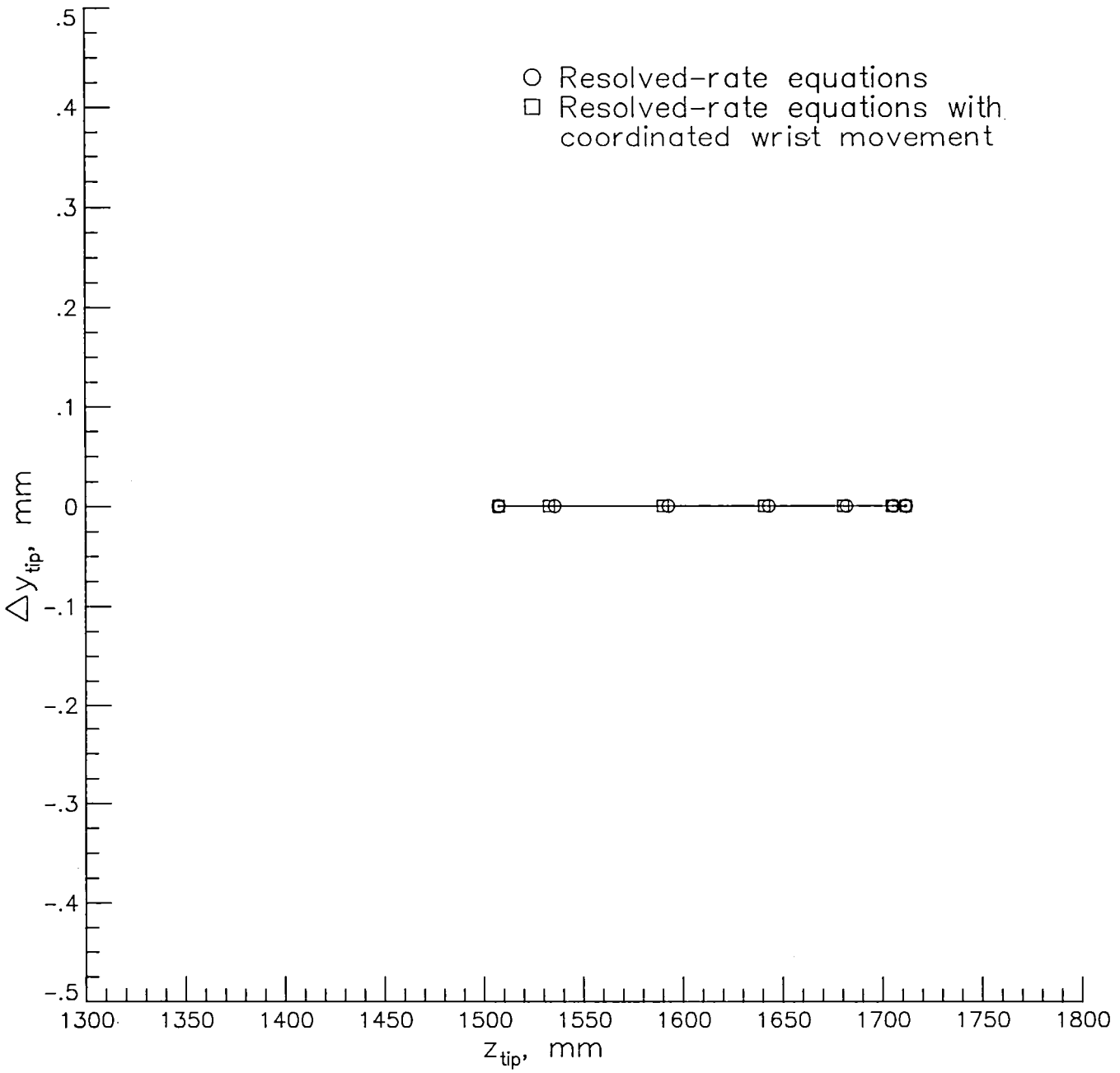

(d) Difference between ideal and actual y_{tip} as a function of z_{tip}.

Figure 5. Concluded.

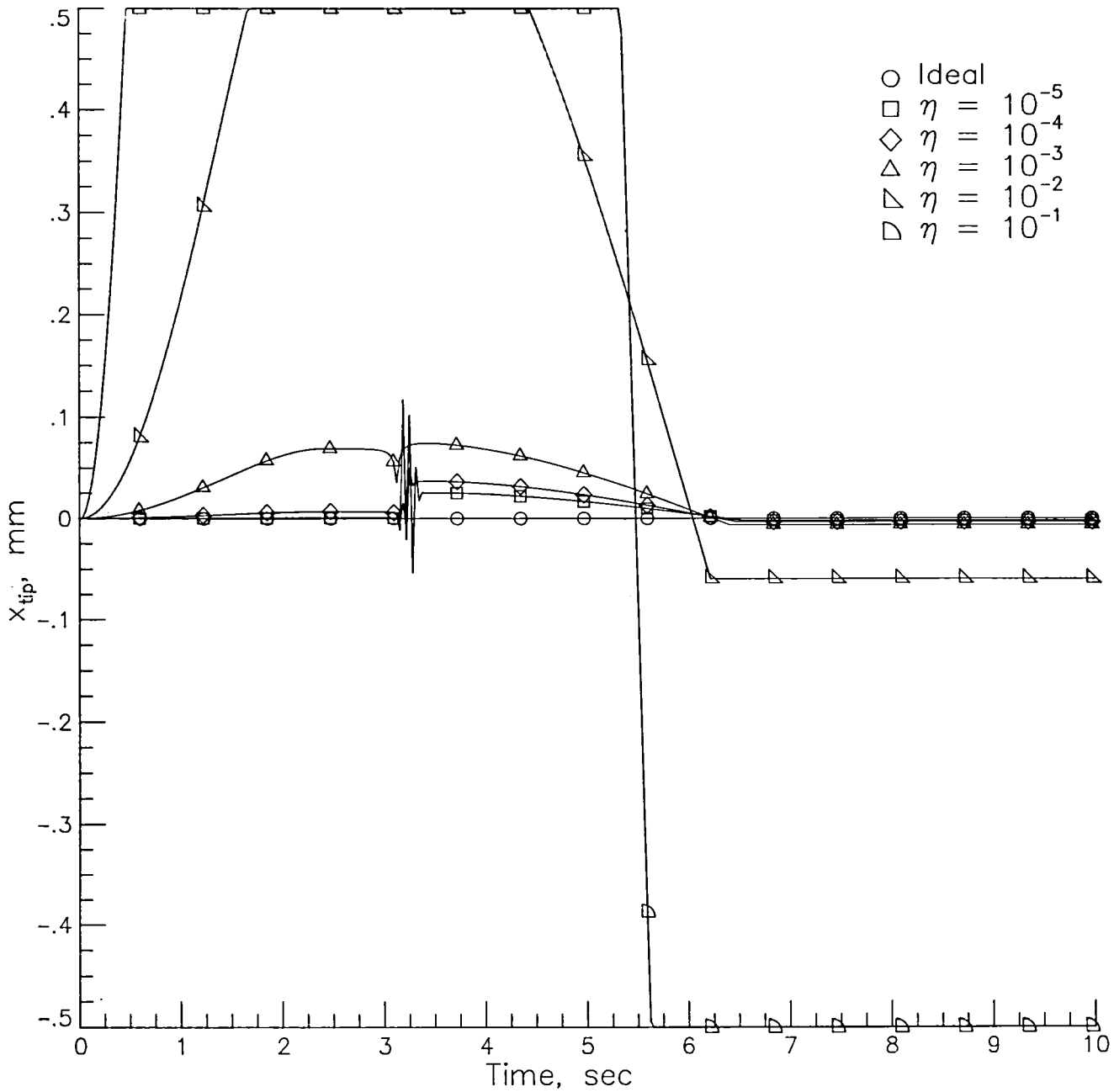

Figure 6. Variation of probe tip x-coordinate with different dead-band values in resolved-rate equations during test maneuver.

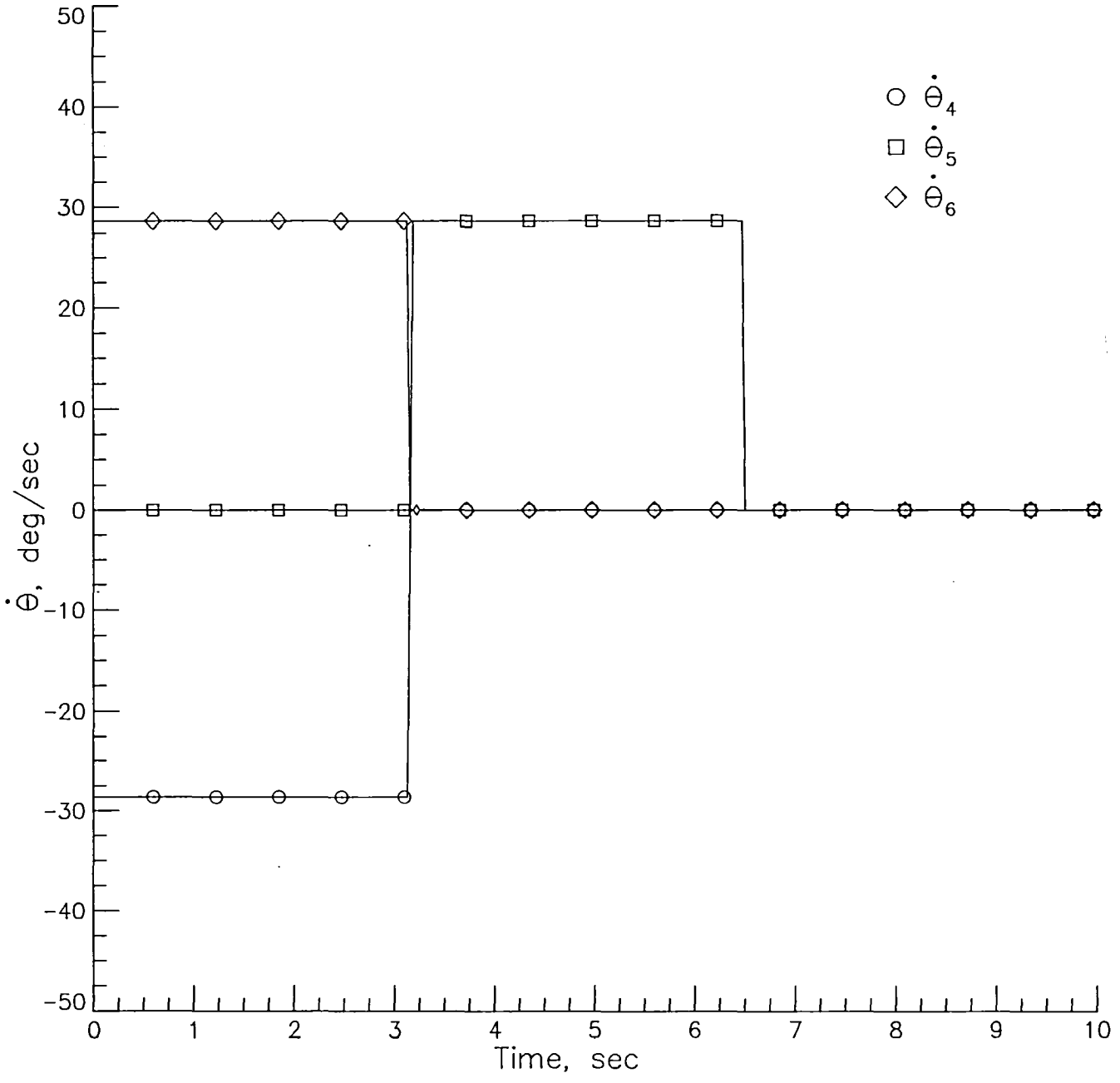

(a) Joint angle rates.

Figure 7. Joint angle rates and joint angles during test maneuver using resolved-rate equations with coordinated wrist movement. $\eta = 10^{-5}$.

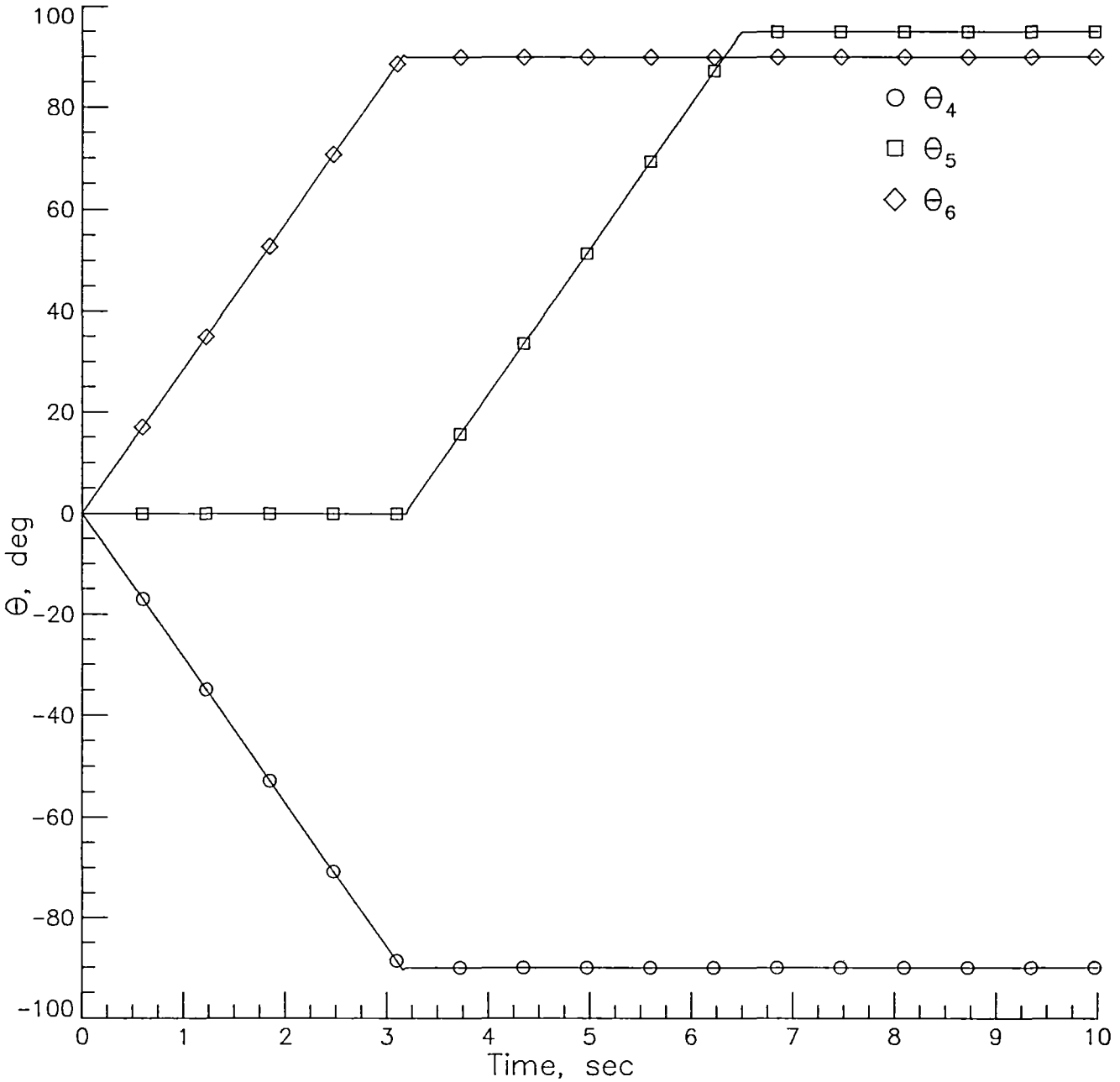

(b) Joint angles.

Figure 7. Concluded.

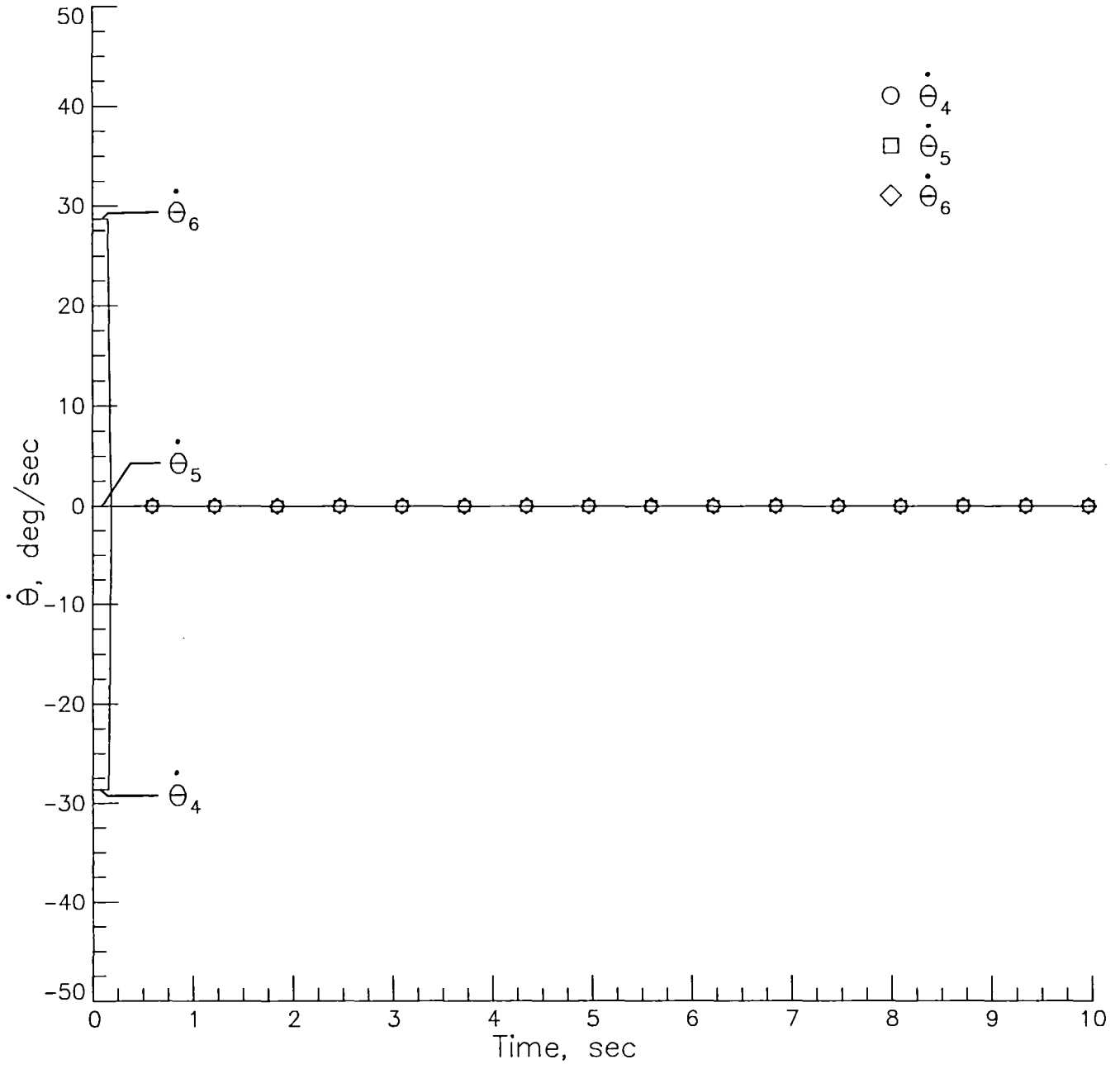

(a) Joint angle rates.

Figure 8. Joint angle rates and joint angles during test maneuver using resolved-rate equations. $|\theta_4| \leq 135°$; initially, $\theta_4 = -130°$; $\eta = 10^{-5}$.

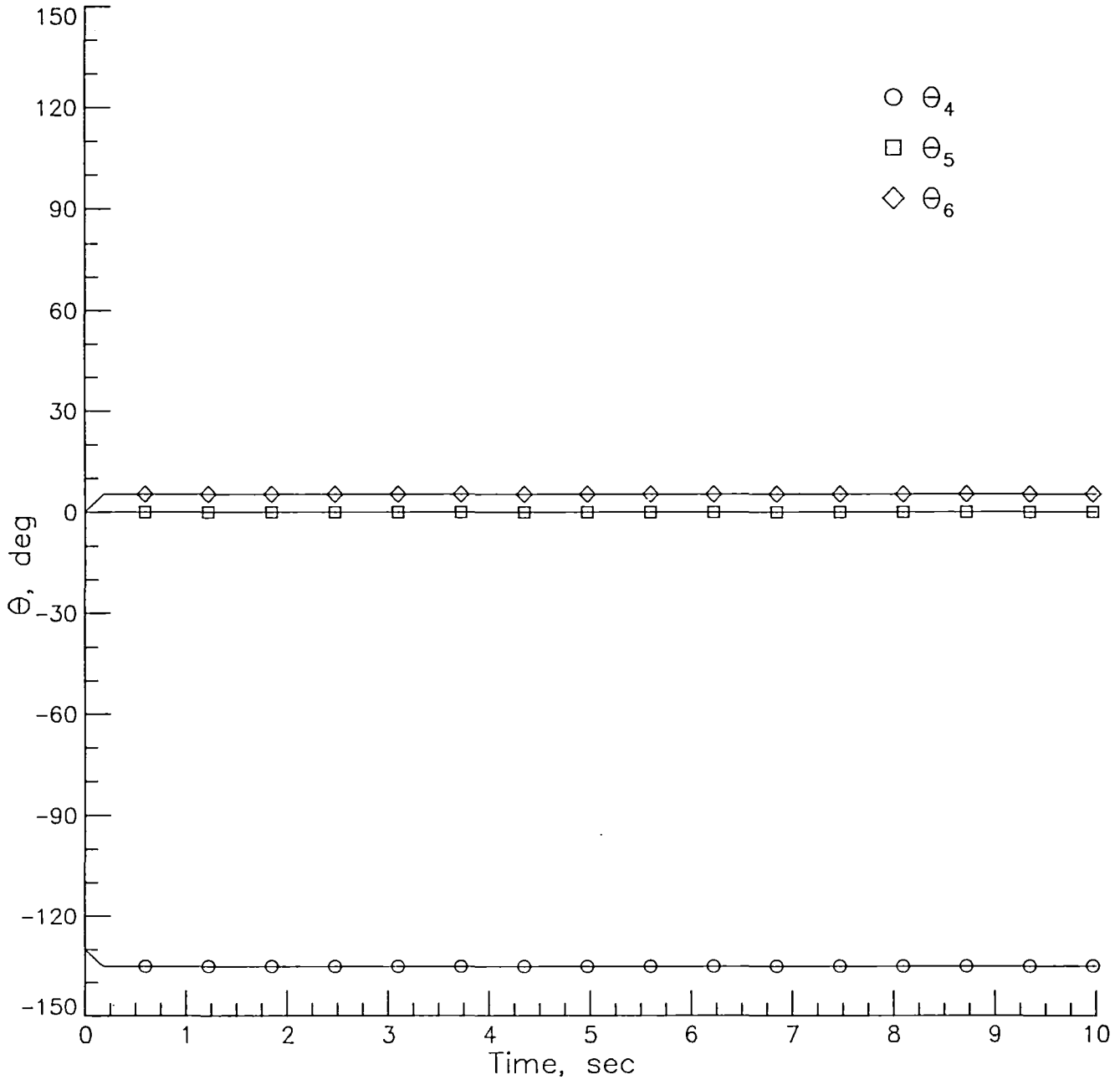

(b) Joint angles.

Figure 8. Concluded.

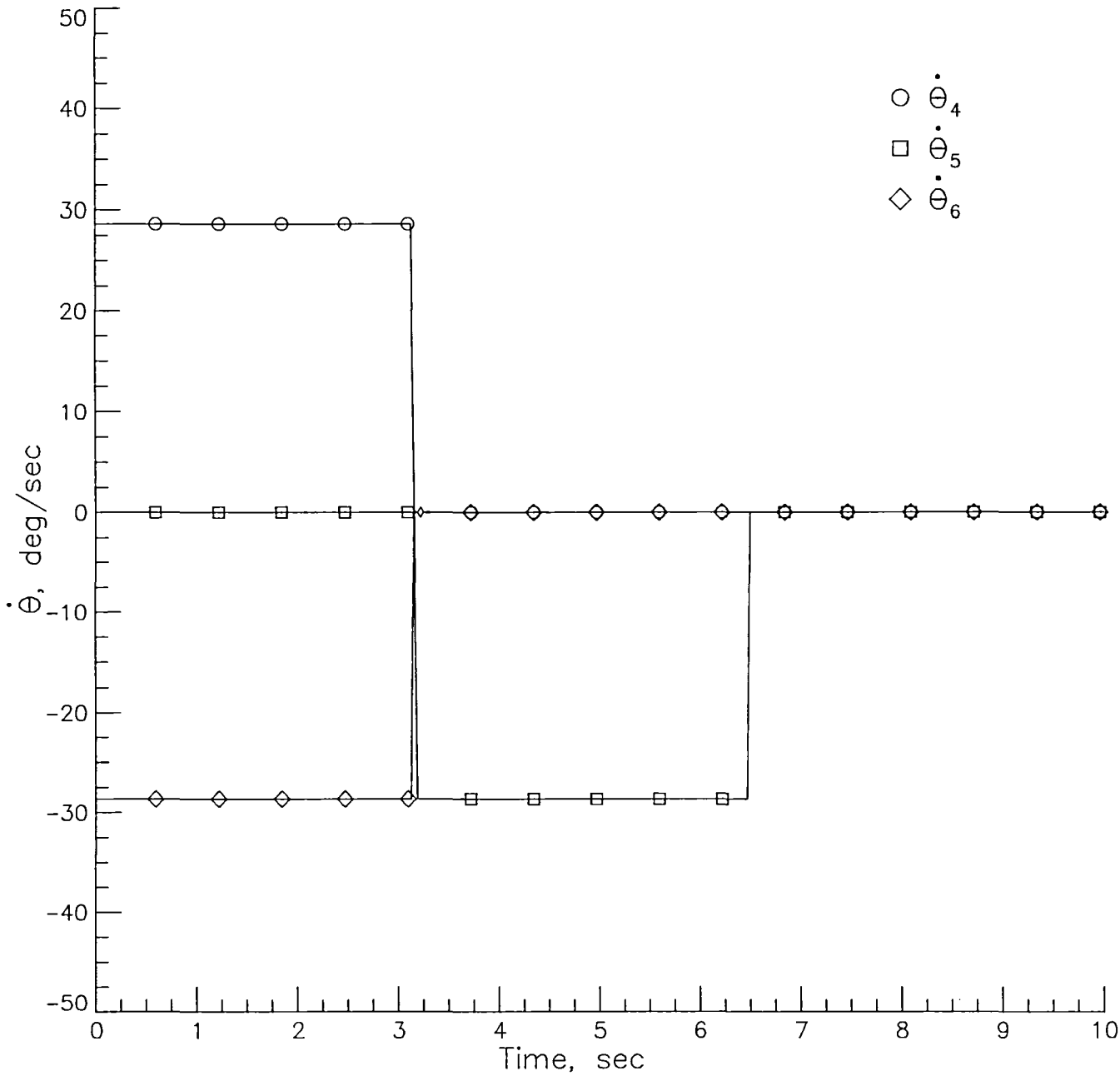

(a) Joint angle rates.

Figure 9. Joint angle rates and joint angles during test maneuver using resolved-rate equations with coordinated wrist movement. $|\theta_4| \leq 135°$; initially, $\theta_4 = -130°$; $\eta = 10^{-5}$.

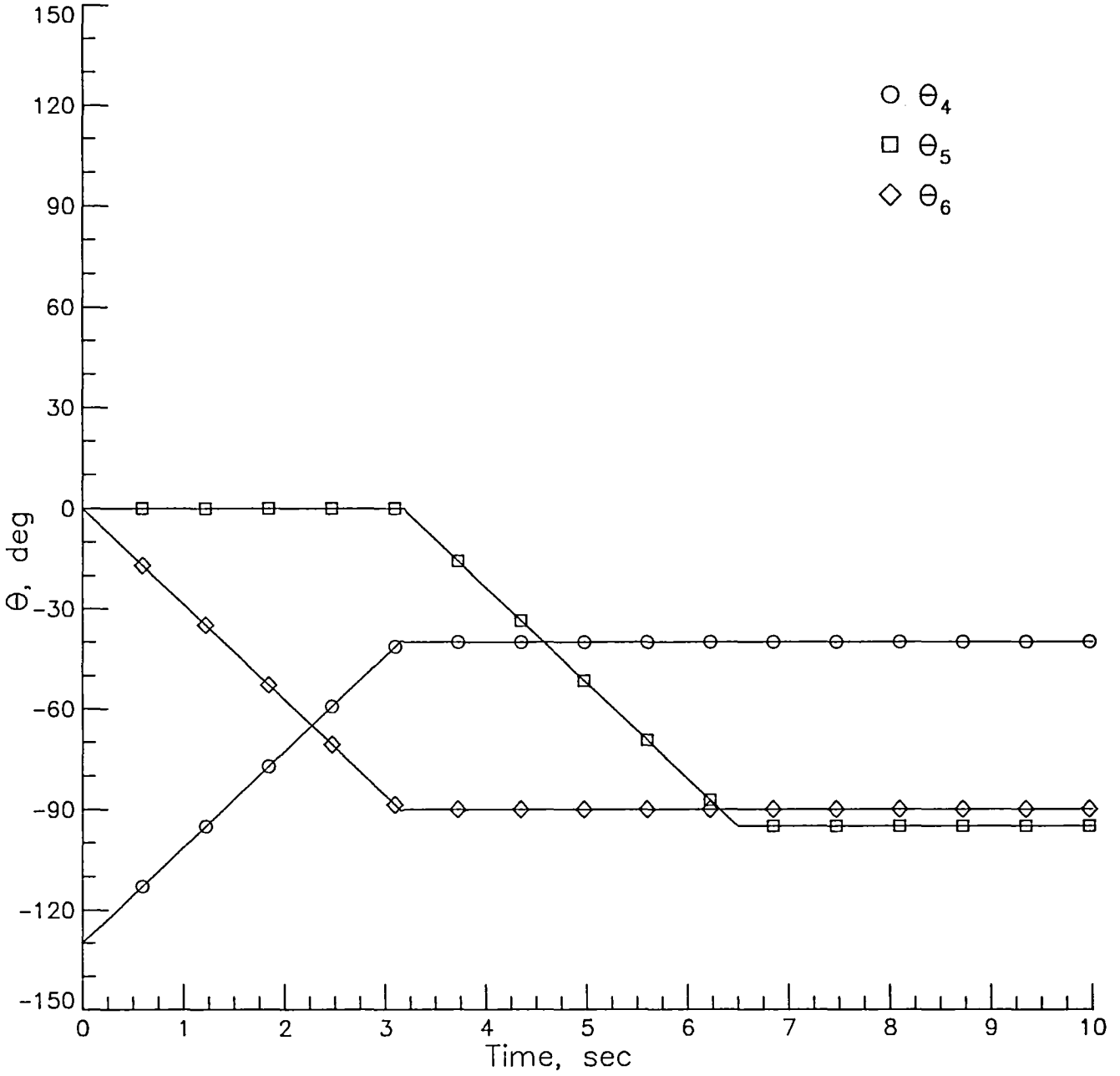

(b) Joint angles.

Figure 9. Concluded.

1. Report No.	2. Government Accession No.	3. Recipient's Catalog No.
NASA TP-2440		

4. Title and Subtitle	5. Report Date
Kinematic Rate Control of Simulated Robot Hand at or Near Wrist Singularity	May 1985
	6. Performing Organization Code: 506-54-63-01
7. Author(s): L. Keith Barker, Jacob A. Houck, and Susan W. Carzoo	8. Performing Organization Report No.: L-15889
9. Performing Organization Name and Address: NASA Langley Research Center, Hampton, VA 23665	10. Work Unit No.
	11. Contract or Grant No.
12. Sponsoring Agency Name and Address: National Aeronautics and Space Administration, Washington, DC 20546	13. Type of Report and Period Covered: Technical Paper
	14. Sponsoring Agency Code

15. Supplementary Notes

L. Keith Barker and Jacob A. Houck: Langley Research Center, Hampton, Virginia.
Susan W. Carzoo: Sperry Corporation, Hampton, Virginia.

16. Abstract

A robot hand should obey movement commands from an operator or a computer program as closely as possible. However, when two of the three rotational axes of the robot wrist are colinear, the wrist loses a degree of freedom, and the usual resolved-rate equations (used to move the hand in response to an operator's inputs) are indeterminant. Furthermore, rate limiting occurs in close vicinity to this singularity. An analysis in this paper shows that rate limiting occurs not only in the vicinity of this singularity but also substantially away from it, even when the operator commands rotational rates of the robot hand that are only a small percentage of the operational joint rate limits. Therefore, joint angle rates are scaled when they exceed operational limits in a real-time simulation of a robot arm. Simulation results show that a small dead band avoids the wrist singularity in the resolved-rate equations but can introduce a high-frequency oscillation close to the singularity. However, when a coordinated wrist movement is used in conjunction with the resolved-rate equations, the high-frequency oscillation disappears.

17. Key Words (Suggested by Authors(s))	18. Distribution Statement
Robot arm Robot wrist Manipulator Kinematic equations Resolved-rate control Singularities Teleoperator Simulation	Unclassified—Unlimited Subject Category 63

19. Security Classif.(of this report)	20. Security Classif.(of this page)	21. No. of Pages	22. Price
Unclassified	Unclassified	26	A03

For sale by the National Technical Information Service, Springfield, Virginia 22161

NASA-Langley, 1985

National Aeronautics and
Space Administration

Washington, D.C.
20546

Official Business
Penalty for Private Use, $300

THIRD-CLASS BULK RATE

Postage and Fees Paid
National Aeronautics and
Space Administration
NASA-451

U.S.MAIL

NASA

POSTMASTER: If Undeliverable (Section 158
Postal Manual) Do Not Return